WASHINGTON UNIVERSITY
DEPARTMENT OF PHYSICS
LABORATORY FOR ULTRASONICS
St. Louis, Missouri 63130

"Quantitative Non-Destructive Evaluation of Composite Materials Based on Ultrasonic Parameters"

Semiannual Progress Report: September 15, 1986 - March 15, 1987

NASA Grant Number: NSG-1601

Principal Investigator:

Dr. James G. Miller
Professor of Physics

The NASA Technical Officer for this grant is:

Dr. Joseph S. Heyman
NASA Langley Research Center
Hampton, Virginia

I. INTRODUCTION

This Progress Report summarizes our continuing research into the non-destructive evaluation of advanced reinforced composite laminates. In previous reports we have described results obtained from such techniques as phase-insensitive C-scan attenuation measurements and polar backscatter measurements applied to the characterization of fatigued and impact damaged composites. In Section II we describe our current research designed to extend this work. In section III we describe our continuing investigations of the applicability of the Kramers-Kronig equations to the nondestructive evaluation of composite materials.

II. INTERROGATION OF FATIGUED AND IMPACT DAMAGED COMPOSITES VIA TRANSMITTED SHEAR WAVES

IIA. INTRODUCTION

In previous Progress Reports this Laboratory has reported on techniques which can be applied to the problem of interrogation and characterization of fiber reinforced composites. One goal in the use of each technique is to obtain a single robust parameter from which the integrity of the scanned samples can be determined. These parameters were then displayed in a gray scale format to allow the investigator a visual means of judging the integrity of the material under investigation. After a brief review of previously reported approaches, we describe the results obtained with a promising new technique.

In our Progress Report covering the period 9/15/81 to 3/15/82 we described the procedure for acquiring a phase-insensitive transmission C-scan, at perpendicular incidence, of a reinforced graphite-epoxy composite. Ultrasonic waves propagating through such inhomogeneous media suffer wavefront distortions due to the differences in velocities and densities of the epoxy matrix and the graphite fibers as well as from irregularities due to damaged regions within the media. The choice of a phase-insensitive receiver was chosen to minimize the effects of phase cancellation across the face of the receiving transducer in an effort to obtain a more accurate estimate of the energy in the transmitted beam. Conventional C-scan measurements based on ultrasonic amplitude contain an offset factor due to the non-zero reflection coefficient at the water/composite interface. Because the slope of the signal loss is independent of reflection coefficient losses, for measurements are made at normal incidence, slope was chosen as the measurement parameter for this study.

The technique of applying polar backscatter as a tool for selectively interrogating plies of a single orientation in a multi-layer composite material was reported in the 3/15/82 to 9/15/82 Progress Report. The power spectrum of the backscattered signal was obtained using an analog spectrum analyzer. This power spectrum was then normalized to the power spectrum obtained in a second (calibration) measurement in which the sample was replaced by a nearly perfect (stainless steel) ultrasonic reflector. The result of this

normalization is the backscatter transfer function, S(f). The backscatter transfer function is a relative measure of the backscattering efficiency at a given frequency. Since frequency averaging over a broad bandwidth reduces the degrading influence of phase cancellation and other interference effects which can compromise the results of backscatter measurements, the frequency average of the backscatter transfer function, termed the integrated backscatter, was chosen as the measurement parameter for these investigations.

Previously reported results from applying these two techniques to a sample which was first fatigued and then impacted (sample E.9.7) are displayed in Figures(1,2). Since the C-scan technique insonifies the sample at normal incidence, the ultrasonic beam is perpendicular to every ply orientation in the specimen. Thus, ply by ply information is lost in this experimental arrangement and a composite image is the result. In Figure(1) a significant area of increased slope of signal loss is indicated in the impact damaged region. The quasi-circular structure suggests a distinct +45° orientation.

The polar backscatter method allows the interrogation of the sample on a ply by ply basis because the strength of the backscattered signal is a function of the azimuthal angle ϕ. Figure(2) displays previously reported results for this mode of interrogation. In Figure(2d) corresponding to a transducer orientation perpendicular to the +45° ply, a region of increased backscatter parallel to this fiber orientation is evident. In panel (c) of Figure(2) (perpendicular to the 0° ply) a circular region of increased backscatter can be seen. Panel (b) (perpendicular to the -45° ply) displays a slightly elevated backscattered signal, but in panel (a) there is little evidence of structure in the region of impact.

The two techniques described above differ not only in the choice of measurement parameter but also on the interrogating probe. The C-scan measurements, because of insonifying the samples at perpendicular incidence, employed longitudinal waves for interrogation. The polar backscatter measurements were obtained with the transducer oriented at a polar angle of 29°. For graphite-epoxy composites this polar angle is past the critical angle for the generation of longitudinal waves. Thus, shear waves were the dominant interrogating mode used for this experimental configuration (due to mode conversion at the water/composite interface). The present work represents a significant extension of the use of shear waves to the interrogation of composite laminates subjected to fatigue and impact damage.

IIB. SAMPLE PREPARATION

The sample chosen for our initial study(E.9.7) is a 1 mm thick eight-ply quasi-isotropic graphite epoxy composite. This composite was fabricated with a ply layup of $[+45/0/-45/90]_s$. The specimen was first fatigued, by subjecting it to 250,000 cycles of expansion and compression at 2/3 of the ultimate strength parallel to the zero degree fibers, then it was impacted with a 1.6 cm diameter steel ball dropped from a height of 4.5 meters.

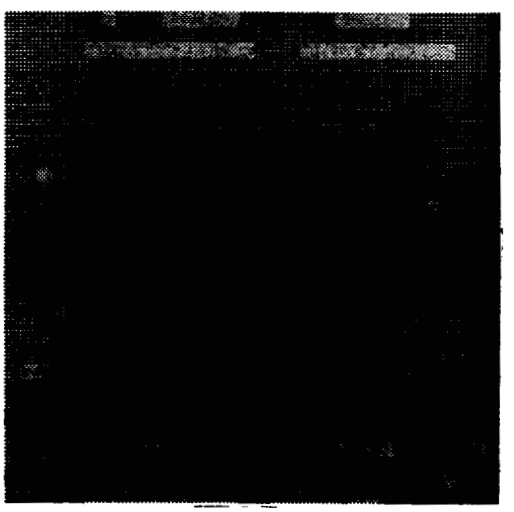

Figure 1: Gray scale image of the slope of the attenuation for the sample E.9.7; initially fatigued, then impacted.

2a) 90 degrees

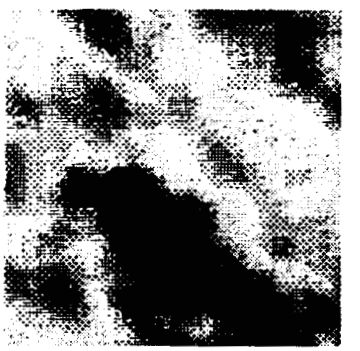

2b) -45 degrees

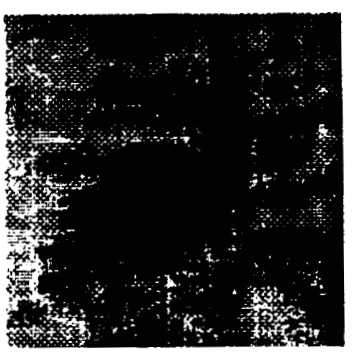

2c) 0 degrees

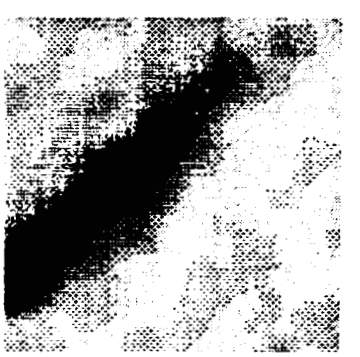

2d) +45 degrees

Figure 2: Gray scale image of the integrated backscatter for the sample E.9.7; initially fatigued, then impacted.

IIC. EXPERIMENTAL METHODS

In Figure(3) we present a schematic diagram illustrating the experimental arrangement for our initial investigation into the interaction of transmitted (rather than backscattered) shear waves with damaged regions in multi-ply graphite-epoxy laminates. For both the transmitting and receiving transducer we chose a 4 inch focused, 0.5 inch diameter, 5 MHz. center frequency, V309 series Panametrics transducer. The polar angle chosen was 30° with respect to the normal of the sample surface as depicted in Figure(3,4). Because this polar angle is greater than the critical angle for the generation of longitudinal modes, the dominant transmitted mode used for this interrogation was shear waves.

The transmitter and receiver were aligned ultrasonically, while viewing the received signal on a spectrum analyzer, by fixing the transmitting transducer and adjusting the receiver to obtain the maximum signal with the broadest frequency spectrum. A calibration spectrum was taken with the two transducers ultrasonically aligned. The sample was then placed in the focal plane of the transmitter and receiver such that the impacted side of the sample faced the transmitter. We insonified a region of the sample far from the site of impact and proceeded to realign the receiver to maximize the signal and minimize the sharp cuts in the power spectrum. Negligible effects were observed from this realignment. This seems plausible since for a 1 mm thick sample refraction and beam deflection effects should be small (in comparison with the 0.5 inch diameter of the piezoelectric receiver we were using for our preliminary measurements). Thus, for our initial investigations we chose to ignore the small spatial shifts due to these effects.

The transmitter and receiver were realigned for the water path only case as described above and a calibration trace was taken. The sample was placed in the focal zones of the transmitter/receiver pair and then raster scanned (in the x,y plane) using the geometry shown in Figure(4). Data were collected over the range from 2 to 7 MHz in 0.02 MHz steps for the water path only calibration trace and for each site in the sample. The data were normalized by employing the method of log spectral subtraction from the calibration trace taken previously, in order to remove the electromechanical response of the measurement system.

The normalized data were analyzed by performing a Taylor expansion around the center of the bandwidth ($f = \bar{f}$),

$$signal\ loss = L(f) = L\big|_{f=\bar{f}} + \frac{dL}{df}\Big|_{f=\bar{f}} \cdot [f-\bar{f}] + \frac{1}{2} \cdot \frac{d^2L}{df^2}\Big|_{f=\bar{f}} \cdot [f-\bar{f}]^2 + \cdots , \qquad (1)$$

where signal loss is in units of dB. We limit our analysis to the first two lowest order terms, consistent with the signal-to -noise ratio exhibited by the data. Equation(1) can be rewritten as

$$signal\ loss\,(f) = K_0 + K_1 \cdot [f-\bar{f}] \qquad (2)$$

$$= average\ signal\ loss + slope \cdot [f-\bar{f}] \ .$$

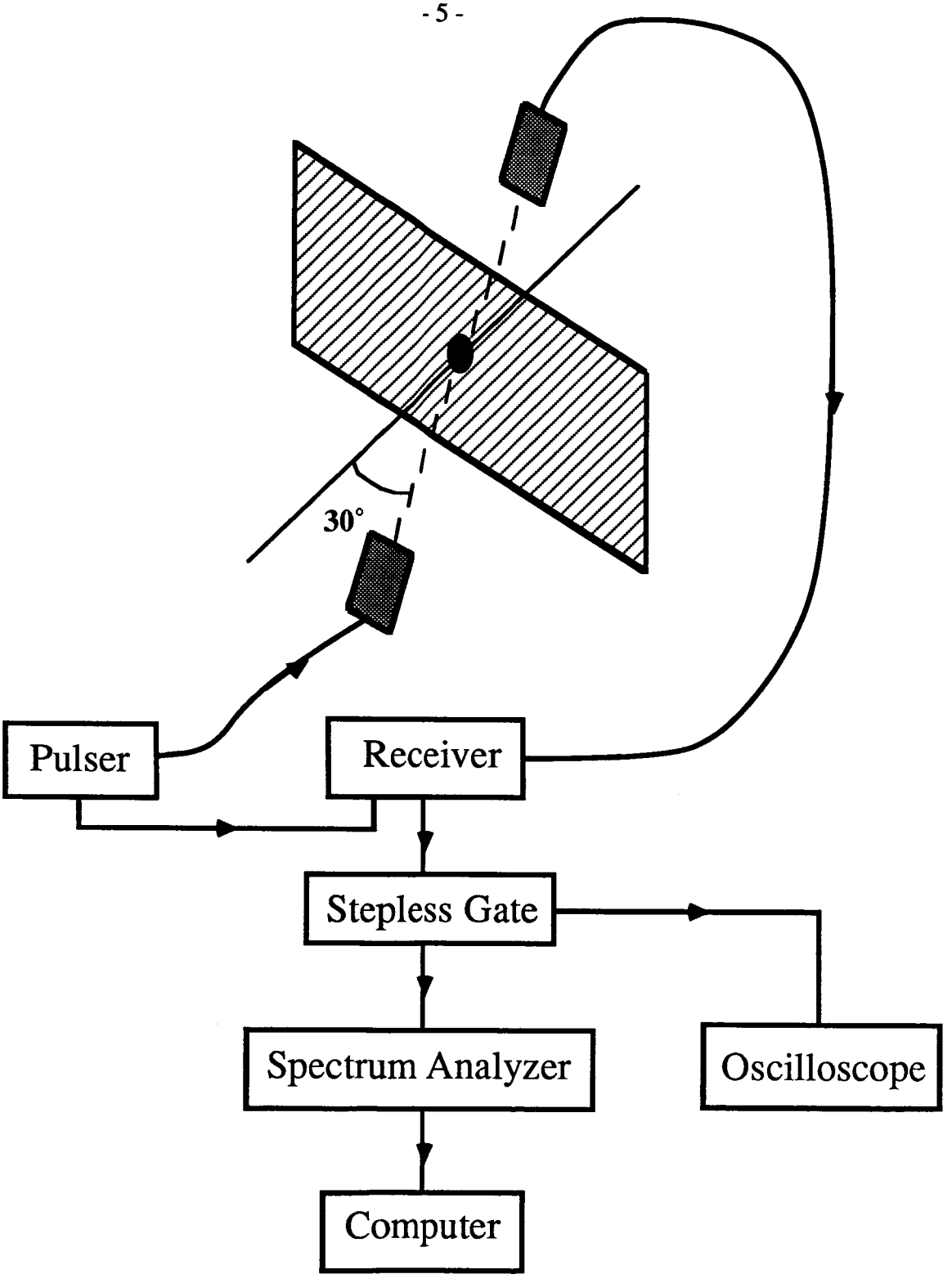

Figure 3: Block diagram illustrating the system used for data acquisition.

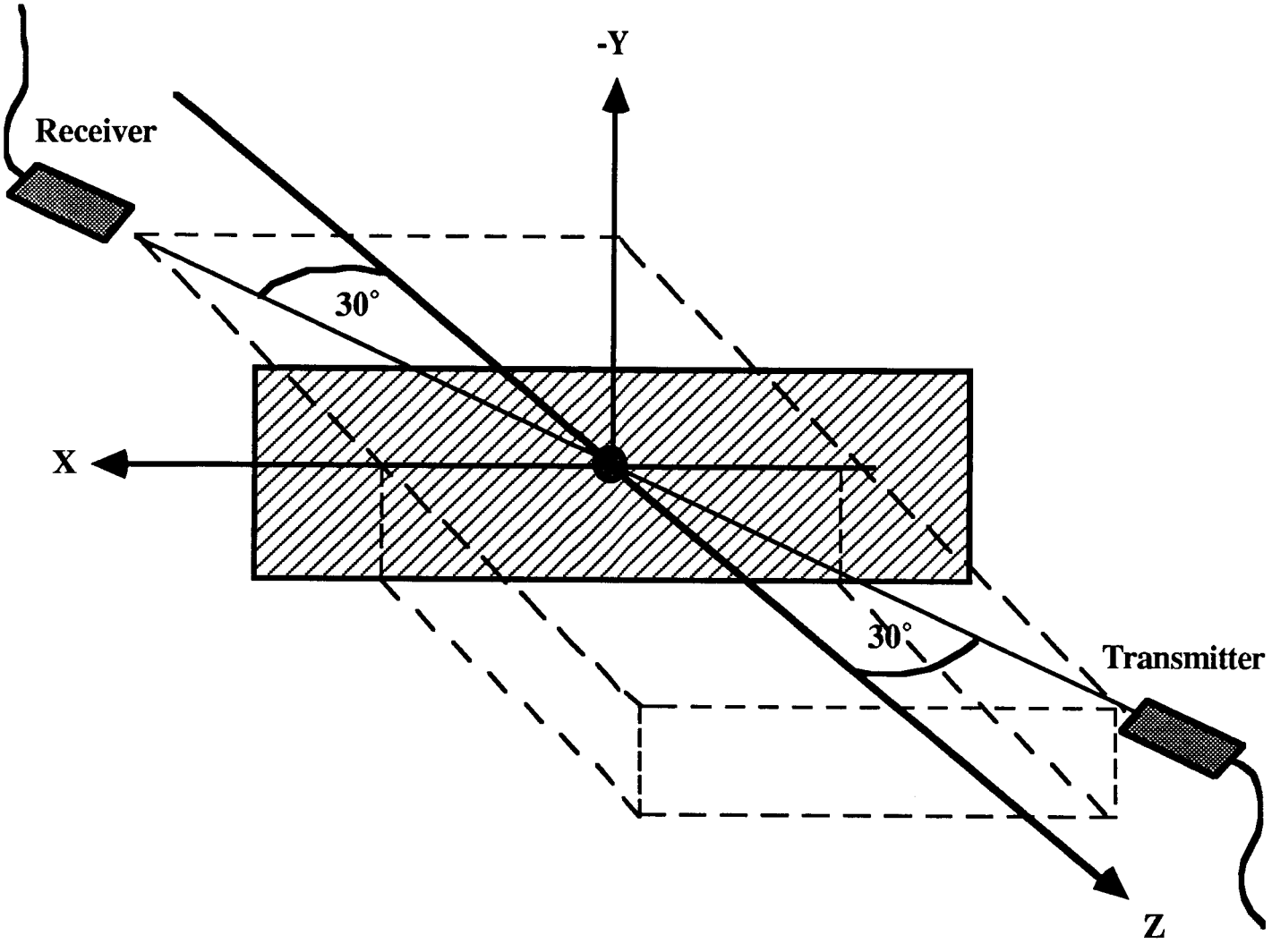

Figure 4: Geometrical arrangement of the sample and orientation of the scanning transducers.

Equation(2) is equivalent to performing a linear least squares fit to the data followed by a linear translation of the coordinate system. The value K_0 of this expansion is an estimate of the average signal loss (dB) over the useful bandwidth, and the slope K_1 is the rate of change of the signal loss (dB/MHz). The calculated values of K_0 and K_1 of the Taylor expansion are each displayed in grayscale format.

IID. RESULTS

In this section the results for our initial investigations into the interaction of transmitted shear waves with fatigued and impact damaged regions of fiber reinforced composites are presented. Figure(5) illustrates the method of Taylor expanding the measured frequency spectrum for a given site about the mean frequency of the useful bandwidth ($f = \bar{f}$). The constant term (K_0) is representative of the average signal loss over the useful bandwidth and the second coefficient of this expansion (K_1) represents the rate of change of this signal loss per MHz.

Figure(6) is a gray scale representation of the calculated slope of the signal loss in dB/MHz along with its associated histogram. The scale ranges from 0.45 dB/MHz for white to 5.1 dB/MHz for black, where each gray level represents 0.14 dB/MHz. The area scanned was 2.0 cm by 2.0 cm in 0.5 mm steps. The image is oriented such that the long axis of the sample, along which the fatigue was applied, is horizontal. The image displays a relatively uniform background with an indication at approximately the center of the scan region. These results may be compared with those obtained by the polar back-scatter method shown in Figure(2).

The *average signal loss* K_0 is displayed in grayscale format in Figure(7). The scale for this image ranges from 11.3 dB for white to 26.0 dB for black, where each gray level represents 0.45 dB. Again we notice a rather uniform background with a indication near the center of the scan region.

One objective of this preliminary study was to ascertain the feasibilty for the use of transmitted shear waves as the interrogating probe in the investigation of fatigued and impact damaged composites. Based on the success of these initial studies, we will conduct careful measurements for angles of incidence corresponding to each of the four fiber orientations. We anticipate that the results of these measurements will provide significant new information because no previous studies have provided data on the attenuation of appropriately polarized transverse waves in regions of fatigue and impact damage.

Measured Signal Loss

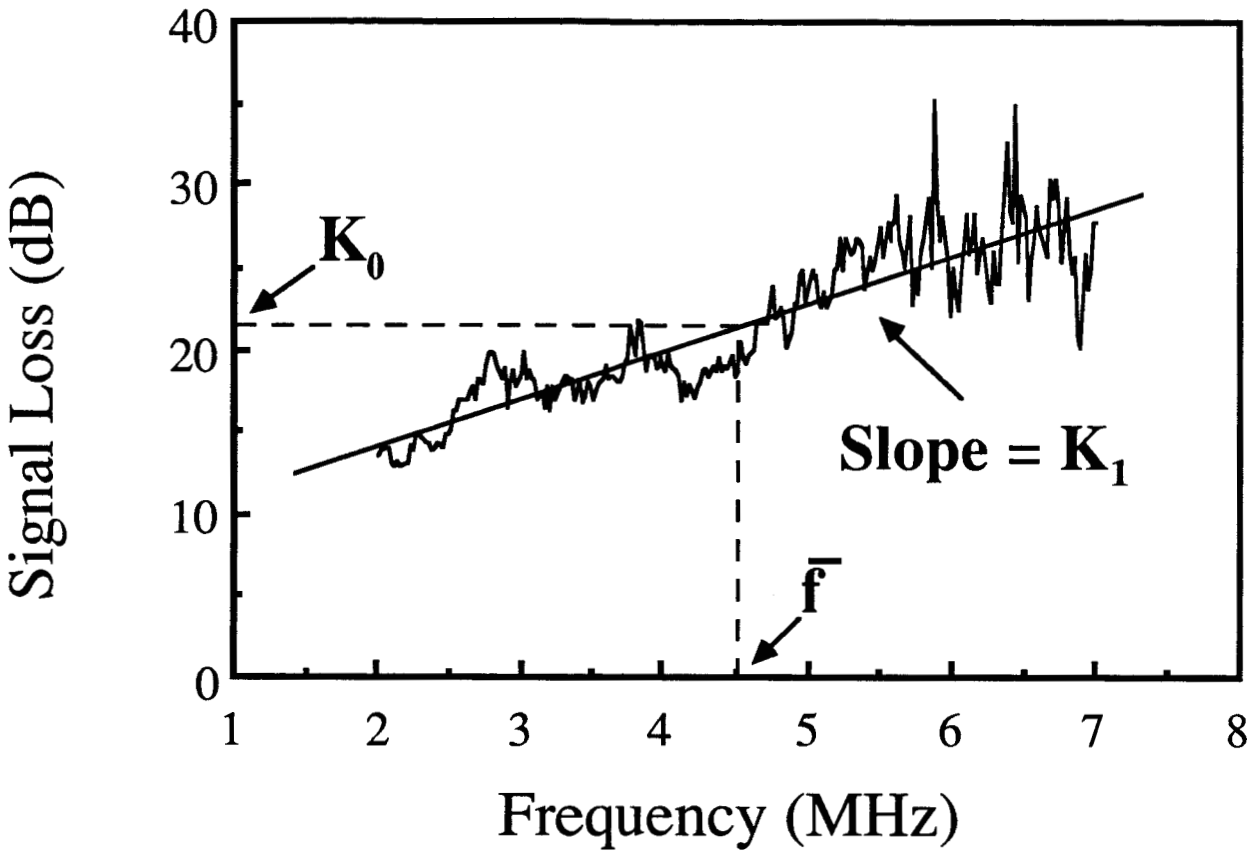

Figure 5: This figure demonstrates the method of Taylor expanding the measured data about the mean frequency ($\bar{f}$). The first two terms of the series correspond to the average signal loss (K_0) over the useful bandwidth and the rate of increase of the signal loss with frequency (K_1).

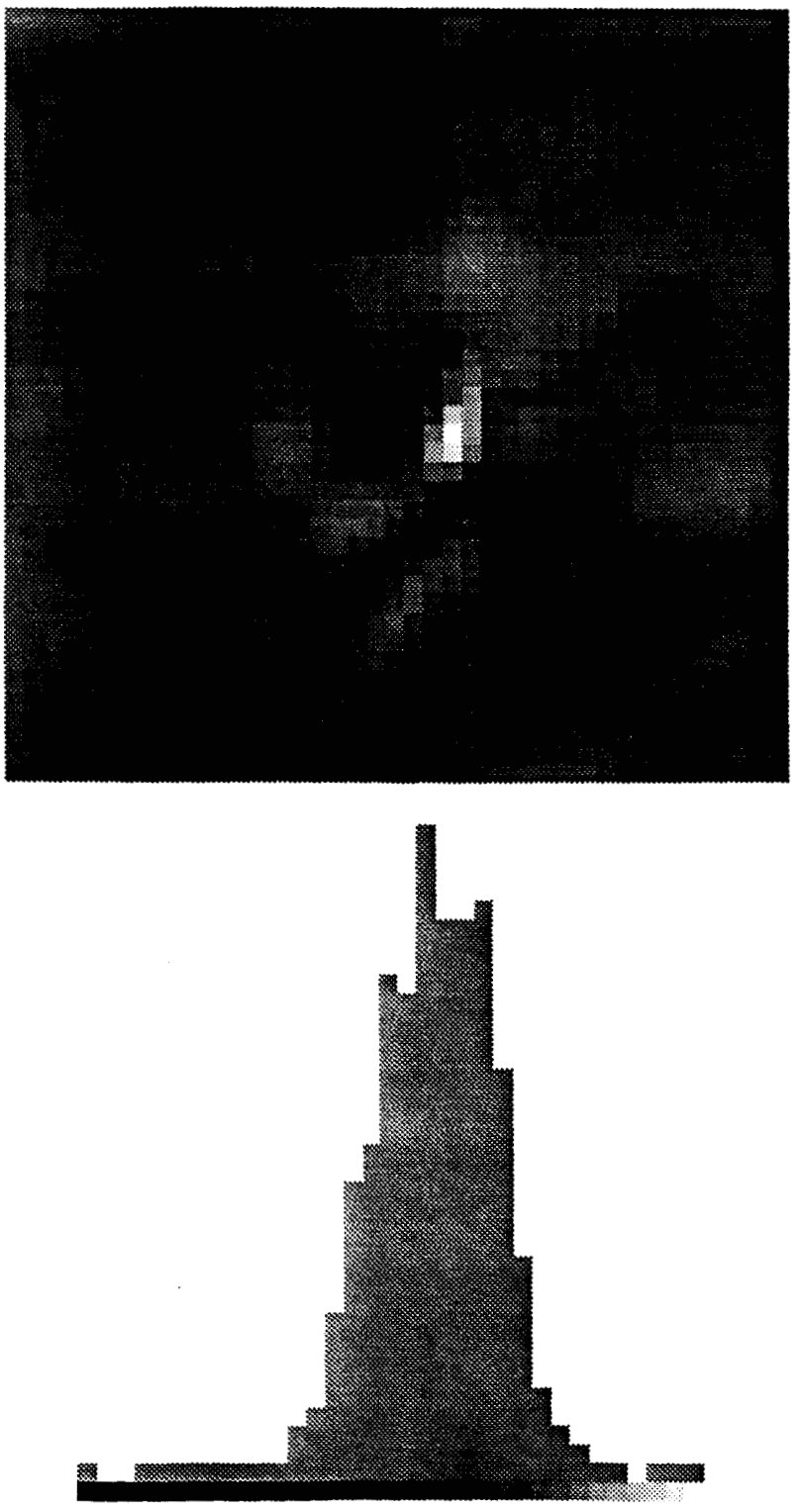

Figure 6: This figure displays the gray scale image and its associated histogram for the slope of the signal loss (K_1) of the fatigued, then impacted sample, E.9.7 (90° orientation).

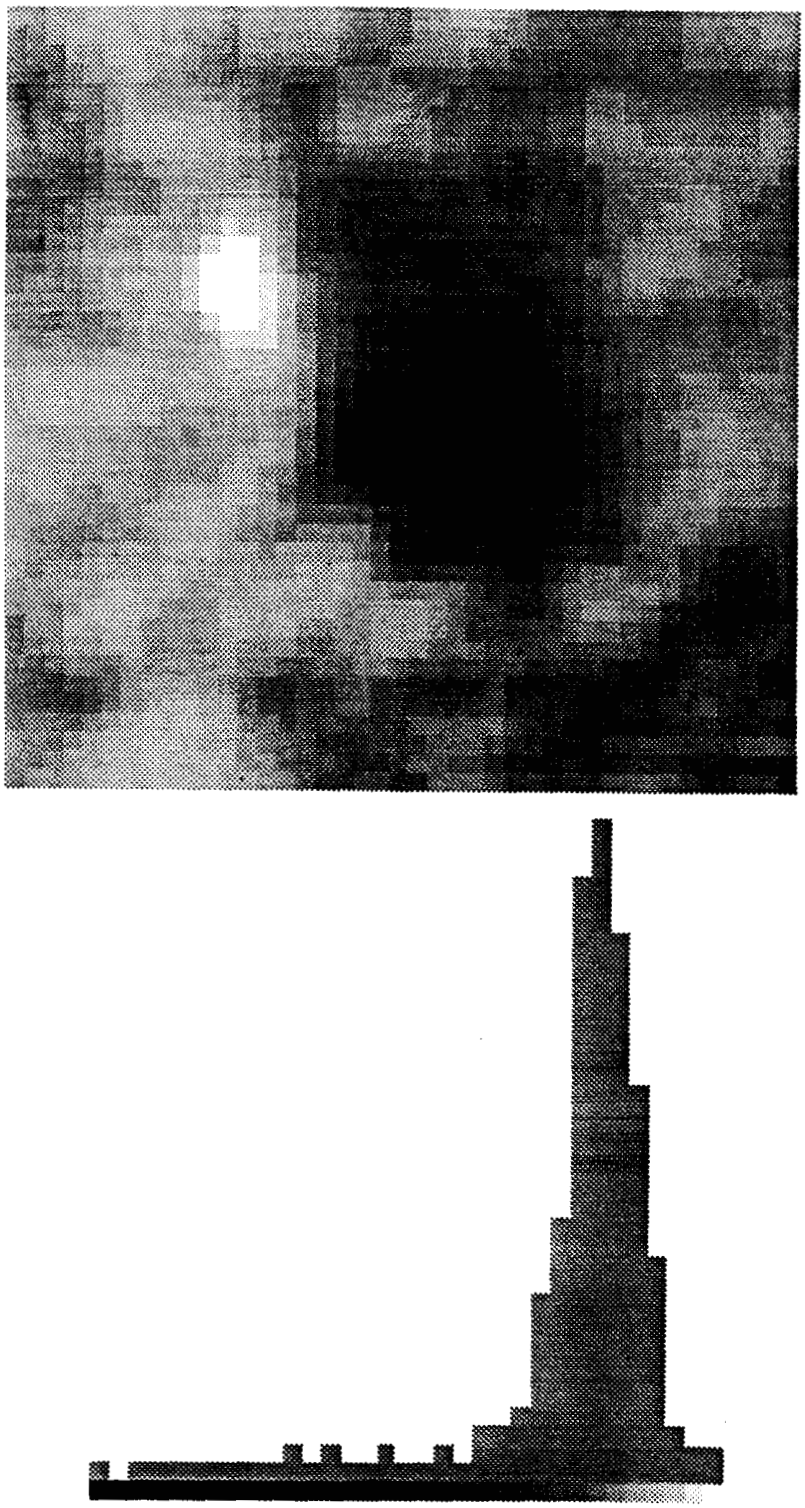

Figure 7: The average signal loss (K_0) is displayed in this figure in gray scale format along with its associated histogram for the sample E.9.7 (90° orientation).

III. CORRELATION OF POROSITY WITH ULTRASONIC PARAMETERS

IIIA. INTRODUCTION

The detrimental effects of voids on the structural properties and lifetimes of composites are well known. Quantitative ultrasonic imaging may provide a reliable nondestructive method for estimating the spatial distribution of porosity or average pore size. A long term goal of this research is to develop ultrasonic techniques capable of establishing that the concentration, average size, and spatial distribution of pores are below some acceptable threshold and thus structurally insignificant.

This section is organized as follows. We first describe the simple model system of "porosity" that was the subject of these preliminary investigations. The ultrasonic apparatus used for the measurement of attenuation and velocity is then discussed. Results of direct measurements of attenuation and velocity as functions of frequency are reported for samples with progressively larger volume fractions of "porosity". Results of the ultrasonic measurements are shown to exhibit a good correlation with the volume fraction of porosity. We then review the role of the Kramer-Kronig relationships connecting ultrasonic attenuation and phase velocity. Data are presented illustrating good correlations between ultrasonic parameters obtained from the Kramers-Kronig relationships and the volume fraction of porosity.

IIIB. SAMPLE PREPARATION

Unidirectional glass fiber reinforced plates were fabricated with several concentrations of glass beads as a simple model of porosity in fiber reinforced composites. Five plates were fabriated, each 5.2 cm by 5.2 cm by 0.3 cm. The glass fibers were approximately 12μm in diameter and four to five cm in length. The fibers ($\rho = 2.43 \pm 0.09$ gm/cm^3) were laid up in an epoxy matrix ($\rho = 1.10 \pm 0.01$ gm/cm^3). Porosity was simulated by the random inclusion of glass beads ($\rho = 2.47 \pm 0.04$ gm/cm^3) drawn from a distribution of radii ranging from 37 μm to 75 μm All samples were fabricated with a fiber volume fraction of $\approx$ 8%. One sample was fabricated without glass beads in order to serve as a control. The remaining four samples exhibited a range of volume fractions of "porosity" ranging from 1% to 12%.

IIIC. MEASUREMENT METHODS

The samples above were placed in a water bath at a temperature of 34° C. The samples were interrogated at perpendicular incidence with ultrasonic pulses from a 10 MHz center frequency, 1/4" diameter, planar transducer. The distance between transducer and sample was 16 cm so that the samples were in the far field of the transducer for all frequencies within the bandwidth of the apparatus. Time domain data were acquired using a Tektronix 2430 digital sampling oscilloscope controlled by a PDP 11/73 computer. Data was later transferred to a Sun 3/160 for computer analysis.

All attentuation data presented in this section of the report were estimated using the log spectral subtraction technique. This technique, which has been described in detail in the 9/15/85 to 3/14/86 Progress Report, is implemented by subtracting the log magnitude of a reflection taken form a nearly perfect stainless steel plate from the log magnitude of a pulse which has propagated through the sample.

Phase velocity was estimated using the ultrasonic spectroscopy technique[1] . Briefly, it requires the computation of the phase of the ultrasonic pulses, acquired in the time domain, as a function of frequency. Knowledge of these phases for pulse which have traveled through the sample as well as for a pulse which has been reflected from a stainless steel reflector allows computation of the phase velocity. This technique has also been described in detail in the Progress Reports covering the periods 9/15/85 to 3/14/86 and 3/15/86 to 9/14/86.

IIID. DIRECT RESULTS vs POROSITY

Both of the techniques described above were used to study the glass-epoxy samples described above. Data were acquired and analyzed for the 1%, 3%, 6%, and 12% samples.

Figure (8) presents the data for the attenuation coefficient as measured in each of the porous composite samples. All samples exhibited an approximately linear frequency dependence for the attenuation coefficient. Futhermore, the slope of attenuation increased with increasing porosity. The frequency range shown for the 6% and 12% samples is roughly half of that shown for the 1% and 3% samples. This smaller useful bandwidth is due in part to the higher attenuation exhibited by these samples.

In order to investigate how the attentuation coefficient depends on the porosity, a straight line was fit to each curve shown in Fig.(8). The slopes of each of these lines were then plotted against porosity. The result of this comparison is shown in Fig.(9). Horizontal error bars represent the uncertainty in the volume fraction of "porosity". Vertical error bars for the slopes of the best fit lines were also calculated but they are too small to be seen on the scale of this graph. The least squares fit line which best fits the data in Fig.(9) was found to be

$$K_1 = 10.6 * \text{concentration} + 0.6$$

with a correlation coefficient of .999.

The phase velocity was also studied as a function of porosity using the technique of ultrasonic phase spectroscopy. For each value of porosity an index of the dispersion (the change in velocity relative to the velocity at 3 MHz) was calculated from the phase velocities. The phase velocity curves obtained for each of the porous glass-epoxy samples are shown in Fig.(11). These curves generally exhibit an increase in dispersion as porosity increases.

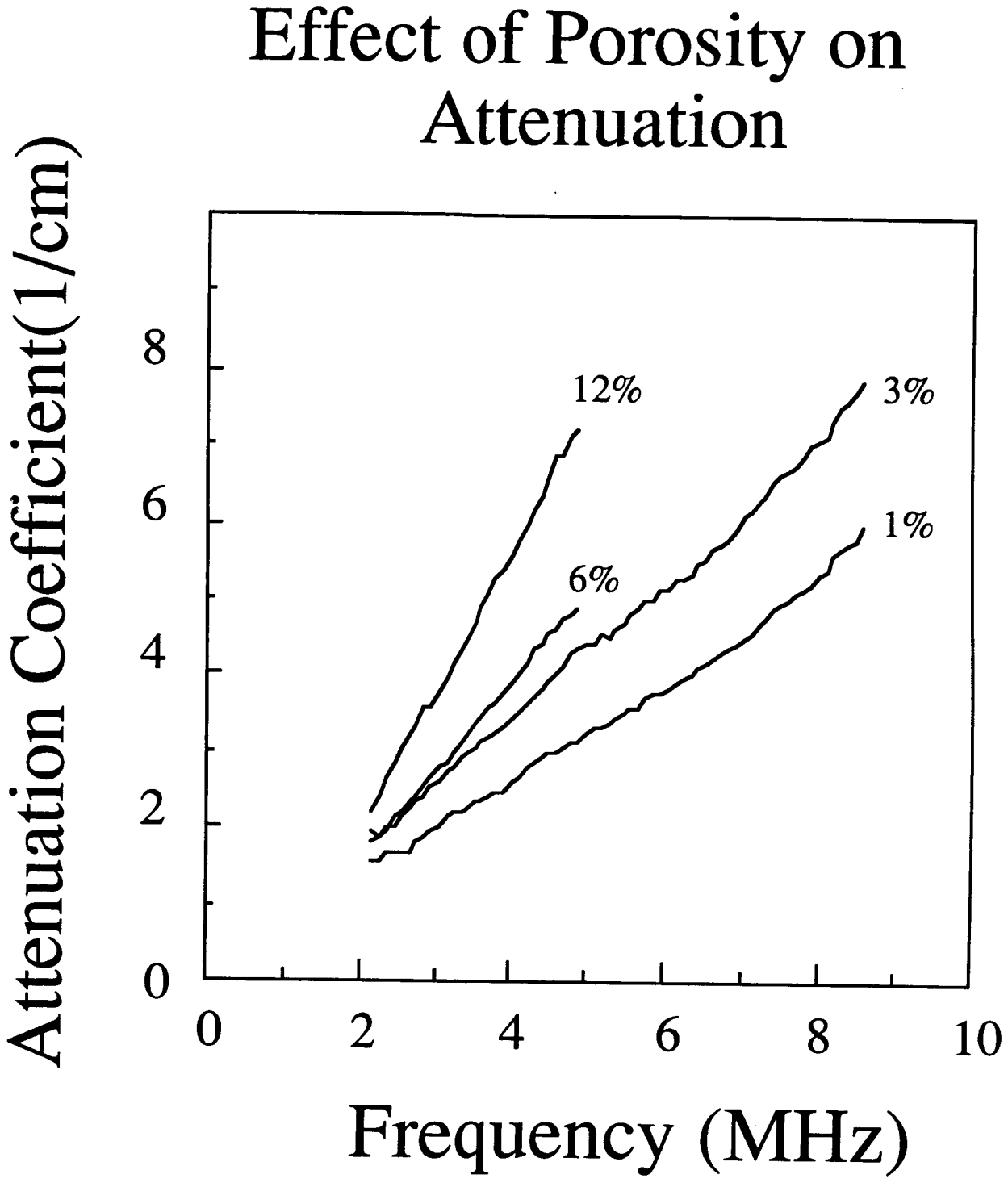

Fig.8 A plot of the attenuation coefficient as a function of frequency for several concentrations of volume fraction of "porosity". The slope of attenuation exhibits an increase with increasing "porosity". Data were acquired in glass epoxy-composite specimens at 34°C. The attenuation coefficient was estimated using the log spectral subtraction technique on data gathered using a shadowed reflector measurement.

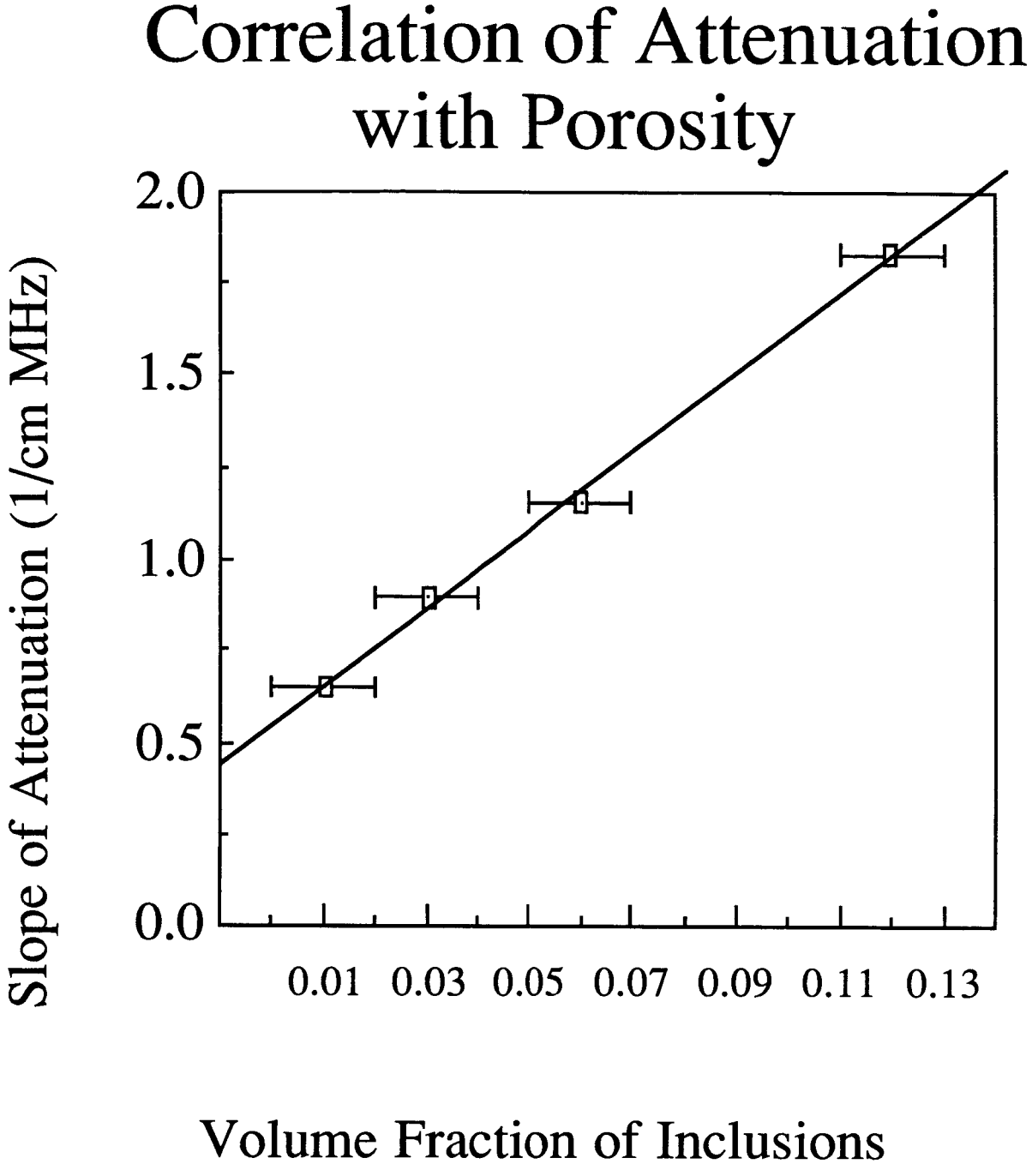

Fig9. Correlation of the slope of attenuation, as estimated directly from experimental data, with the volume fraction of "porosity". The slope of attenuation was obtained using a least squares fit to the experimentally obtained attenuation data. These attenuation data were obtained using a log spectral subtraction technique. All data were obtained in glass-epoxy specimens at a temperature of 34°C.

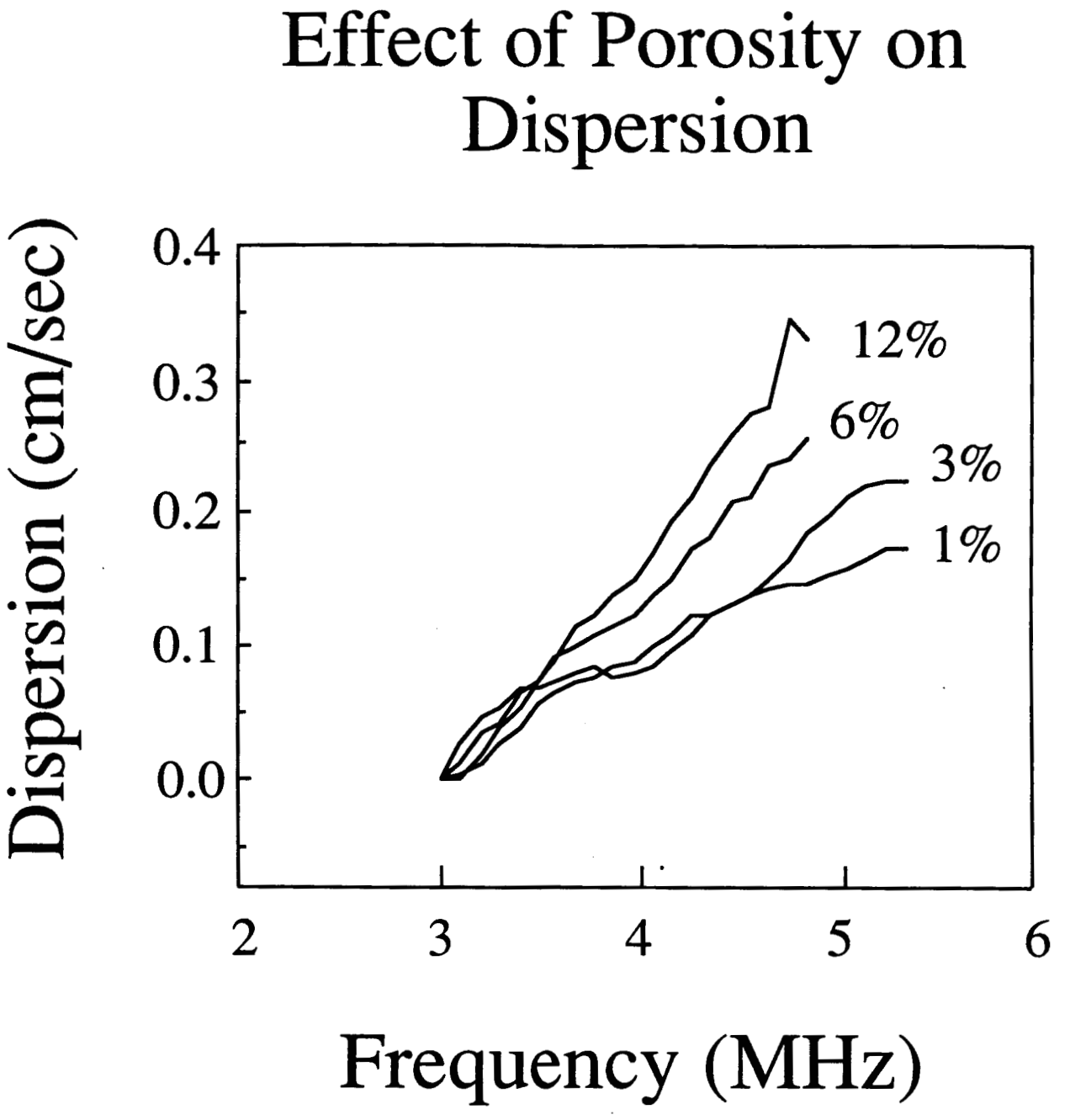

Fig.10 A plot of the dispersion (change in phase velocity expressed relative to the velocity at 3 MHz) as a function of frequency for several concentrations of volume fraction of "porosity". The dispersion exhibits an increase with increasing "porosity". Data were acquired in glass epoxy-composite specimens at 34°C. The dispersion was estimated using the technique of ultrasonic spectroscopy.

The total change in velocity between 3 and 5 MHz is plotted as a function of porosity in Fig.(11). The large horizontal error bars reflect the uncertainty in the volume fraction of "porosity" in each sample. Vertical error bars were also estimated but are too small to be seen on the scale of the graph. The least squares line fit to the data points and shown in the figure has the equation

$$K_1 = 1.6 * \text{concentration} + 0.1.$$

Thus very correlation was obtained between ultrasonic estimates and direct assessment of porosity with a correlation coefficient of .999.

IIIE. KRAMERS-KRONIG RELATIONS AND POROSITY

IIIE.1 Introduction

Previous Progress Reports have focused on the validity of the Kramers-Kronig relations in both homogeneous and inhomogeneous media. In this section we report on the applications of these efforts to the porous glass-epoxy composites described above.

IIIE.2 Theoretical Background

Previous Progress Reports have described results based on the Kramers-Kronig equations for the complex dynamic compressibility $\kappa(\omega)$ of a medium. $\kappa(\omega)$ obeys the following pair of Kramers-Kronig integral equations:

$$\kappa_1(\omega) = \frac{2}{\pi}\int_0^\infty \frac{\omega'\kappa_2(\omega')}{\omega'^2-\omega^2}d\omega' + \kappa_1(\infty) \tag{3}$$

which gives the real part $\kappa_1(\omega)$ of the dynamic compressibility in terms of the imaginary part and,

$$\kappa_2(\omega) = \frac{-2\omega}{\pi}\int_0^\infty \frac{\kappa_1(\omega') - \kappa_1(\infty)}{\omega'^2-\omega^2}d\omega' \tag{4}$$

which gives the imaginary part in terms of the real part. Previous Progress Reports have described local approximations to these equations. The relevant approximation for this report is

$$\kappa_2(\omega) = -\frac{\pi}{2}\omega\frac{d\kappa_1(\omega)}{d\omega} \tag{5}$$

Combining Eq.(5) with the dispersion relationship we obtain the following equation which involves ultrasonic parameters which may be measured with the appartus described in the Measurements section of this report.

$$\alpha(\omega) = \frac{\pi\omega^2}{2C(\omega)^2}\frac{dC(\omega)}{d\omega} \tag{6}$$

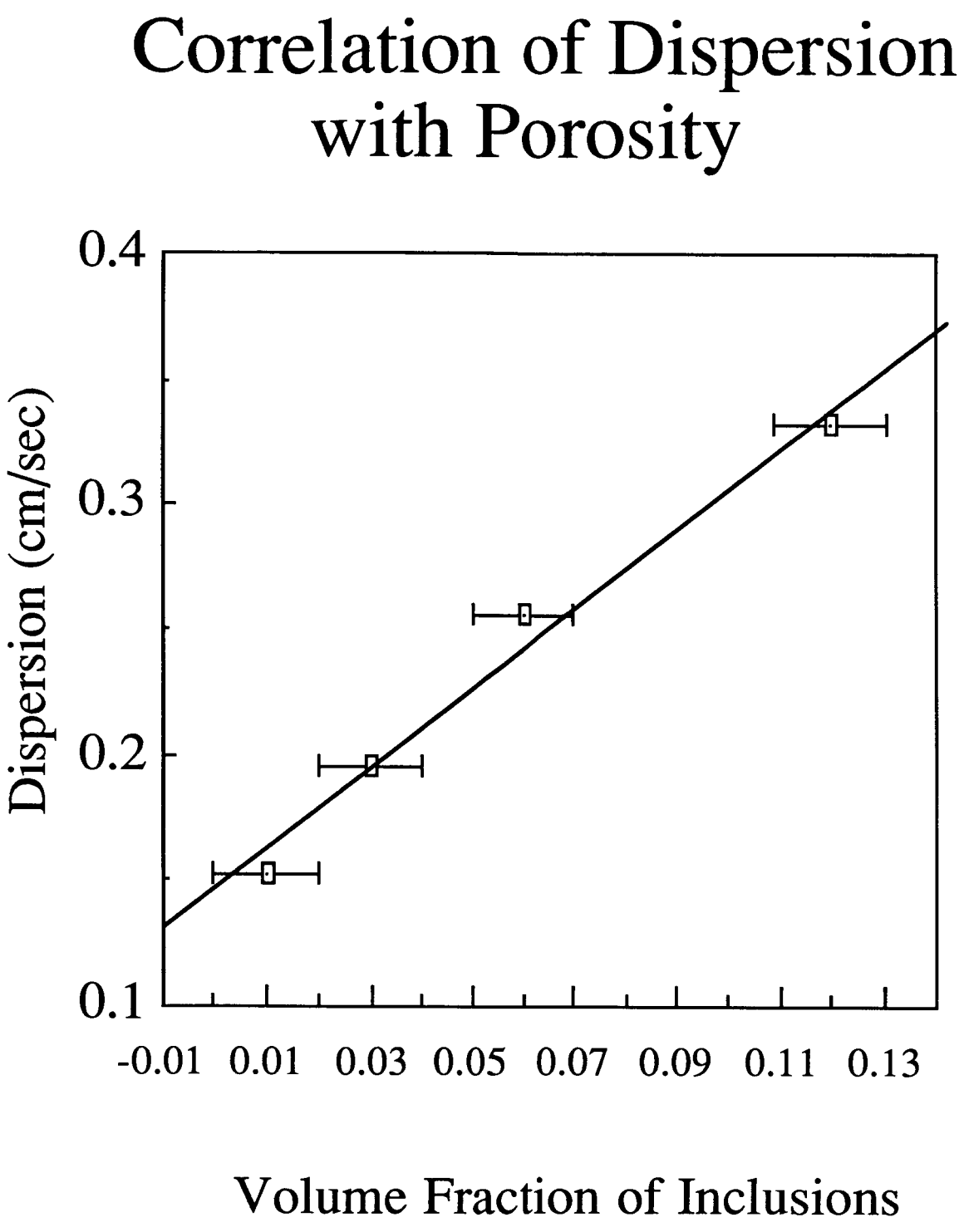

Fig.11 Correlation of the average dispersion, as estimated directly from experimental phase velocity data, with the volume fraction of porosity. The dispersions plotted above were obtained by computing the change in phase velocity between 3 MHz and 5 MHz. All data were obtained with glass-epoxy composite specimens at 34°C.

where $\alpha(\omega)$ is the attenuation coefficient and $C(\omega)$ is the phase velocity. This equation may be integrated to produce the following equation which has the advantage over Eq.(6) in that it is stable in the presence of noise

$$C(\omega) - C(\omega_0) = \frac{2C_0^2}{\pi} \int_{\omega_0}^{\omega} \frac{\alpha(\omega')}{\omega'^2} d\omega' \tag{7}$$

This equation allows the computation of the phase velocity from the experimentally measured attenuation data.

IIIE.3 Results for Kramers-Kronig Estimated of Phase Velocity

Equation 7 was used to compute the phase velocity from the attenuation for all four of the glass-epoxy composites described above. The integral was evaluated using a composite Simpson's rule. This calculated phase velocity was then plotted as a function of porosity. The results of this comparison are shown in Fig.(12). The straight line drawn in Fig.(12) was obtained from a least squares fit and has the form

$$K_1 = 3.2 * \text{concentration} + 0.2.$$

The correlation coefficient for this line is r = 0.99, indicating very good agreement between ultrasonic and direct assessments of porosity.

For attenuation data which are well approximated by a straight line, such as those shown in Fig.(8), there is an alternative procedure for the calculation of Eq.(7). It begins by fitting a straight line to the data for the attenuation coefficient. If the attenuation coefficient is modeled as $\alpha(\omega) = \beta f$ the slope of the fit line gives a good estimate of β . It is then possible to insert this relationshop into Eq.(7) and carry out the integration in closed form and obtain an estimate of phase velocity from the measured values of attenuation coefficient. This procedure was carried out for each of the porous glass-epoxy specimens. The results are shown in Fig.(13). The straight line in this figure was obtained from a least squares fit to the plotted points and has the form

$$K_1=2.6 * \text{concentration} + 0.2$$

with a correlation coefficient of 0.999, again indicating very good agreement between ultrasonic and direct assessments of porosity.

References

1. Wolfgang Sachse and Yih-Hsing Pao, "On the Determination of Phase and Group Velocities of Dispersive Waves in Solids," *J. Appl. Phys.*, vol. 49, pp. 4320-4327, 1978.

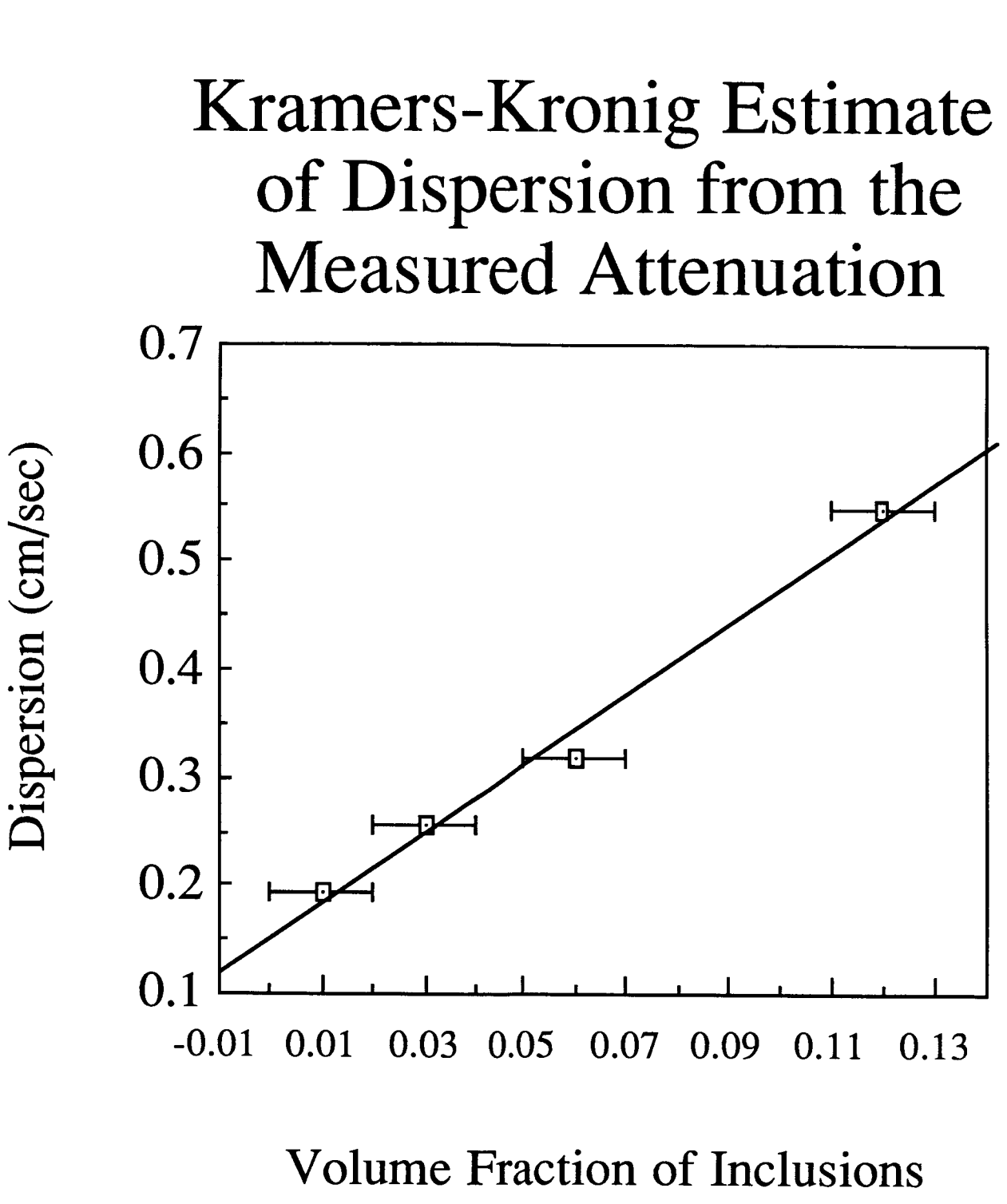

Fig.12 Correlation of the dispersion with the volume fraction of "porosity". The dispersion (change in phase velocity between 3 and 5 MHz) was obtained from the phase velocity as estimated from the attenuation data using the integral form of the local approximation to the Kramers-Kronig relationships. The version shown above makes no assumptions about the frequency dependence of the attenuation coefficient. These data were obtained with glass-epoxy specimens at 34°C..

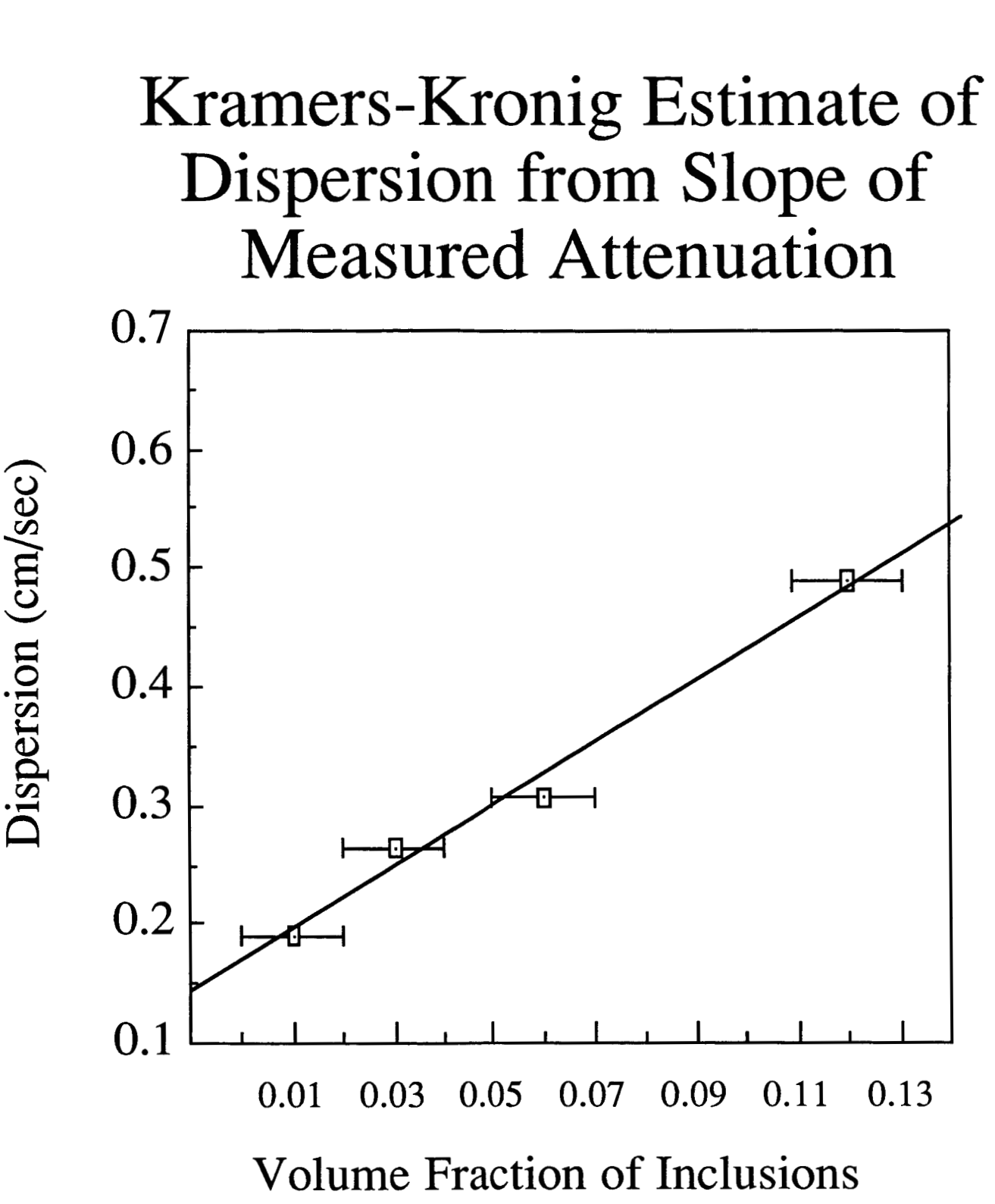

Fig.13 Correlation of the dispersion with the volume fraction of "porosity". The dispersion (change in phase velocity between 3 to 5 MHz) was obtained from the phase velocity as estimated from the attenuation data using a version of the integral form of the local approximation to the Kramers-Kronig relationships. This version of the approximation incorporates the assumption that the attenuation coefficient is a linear function of frequency. These data were obtained with glass-epoxy specimens at 34°C.